QUALITY AND RELIABILITY ENGINEERING INTERNATIONAL, VOL. 10, 217–227 (1994)

# 'ON-LINE' G-CONTROL CHART FOR ATTRIBUTE DATA

ELI A. GLUSHKOVSKY
*TELRAD, P.O. Box 50, Lod 71100, Israel*

SUMMARY

On the basis of the *theory of random processes* the concept of a $G$-chart is elaborated. In this case the observed variable $G$ is a number of conforming units between two consecutive appearances of non-conforming ones. If the process is a Poisson one then $G$-variables are geometrically distributed (the $G$-chart is called after the distribution type). Application of a new SPC concept for attribute data makes it possible to improve SPC employment for: *high quality processes* with $\bar{p} < 10^{-4}$ (100 ppm); *low volume manufacturing, short runs* and *'stepped' processes*. In the paper *individual G, G-bar* and *stabilized* $G/\bar{G}$ charts are presented. The sensitivities of a $G$-chart and a classical $p$-chart for the detection of process changes are compared by constructing operating characteristic curves and ARL curves. Depending on the required degree of the detection process changes, an optimal size of subgroup is found. For this size of subgroup the average number of non-conforming units and the average number of observed units between the process change and this change detection are minimal. Compared with the classical $p$-chart of the same sensitivity, the $G$-chart requires on the average fewer observed units for process change detection and also on the average fewer non-conforming units are produced.

KEY WORDS Attribute data Random process Control chart Control limit Operating characteristic curve

## INTRODUCTION

At present, notwithstanding a wide application of SPC methods for attribute data, there are some areas where their employment is still a problem.

### 1. *High quality processes*

Paradoxically, classical SPC methods for attribute data can be applied only for low quality processes. Why? In these methods the fraction of non-conforming units or defects appearing in a sample is observed. For low probability of non-conforming units it is necessary to go to 100 per cent inspection to ensure the adequacy of SPC functioning and enlarge sample size. For a binomial distribution, the smallest possible value for the lower control limit is LCL = 1, then we have[1]

$$(1-\bar{p})^n < \alpha_L \text{ or } n > \log(\alpha_L)/\log(1-\bar{p})$$

where $\alpha_L = \alpha_U = \alpha = 0{\cdot}00135$ (classical $\pm 3\sigma$ control limits) and $\bar{p}$ is the average fraction non-conforming.

Even if $\bar{p} = 0{\cdot}01$ (10,000 ppm), the sample size must be $n > 660$, but now for some processes we have $\bar{p} < 10^{-4}$ (100 ppm) for which $n > 66{,}100$. Thus, from the point of view of response dynamics these methods are shifted from the 'on-line' class to 'off-line' one with the quality improvement.

### 2. *Low volume manufacturing, short runs*

This is the other side of the same problem for high quality processes. But the cause is disparity between lot and required sample size. What can be done if the sample size must be $n > 660$ and the whole production lot is 300 units?

### 3. *'Stepped' processes*

In these processes the observed attribute is 'good/OK' from the beginning till a certain moment, after which it becomes 'bad' for all following observations.

Here are some of such processes:

(a) *Chemical, thermodynamical processes* with the changing properties of materials, catalysts.
(b) *Processes connected with wear or breakage of instruments*. For example, drilling with a 'go/no-go' inspection. The appearance of the first non-conforming unit means the wear or the breakage of the drill. Another example is a punch process when we are observing the appearance of notches.

Formally, 'stepped' processes can be described by a non-symmetrical stepped function:

$$U(\text{Arg}-\text{Var}) = \begin{cases} 1, & \text{'bad' state, } \text{Arg} \geq \text{Var} \\ 0, & \text{'OK' state, } \text{Arg} < \text{Var} \end{cases} \quad (1)$$

where Var = $\{W, T\}$, the number $W$ of units or the time interval $T$ from the beginning till the first non-conforming unit appearance, and Arg = $\{w, t\}$, the current number $w$ of units appearance or the time $t$.

Control of these processes makes it possible to improve the quality of instrument preparation,

CCC 0748–8017/94/030217–11


*Received 20 June 1993*
*Revised 10 February 1994*

machine adjustment, materials utilization and environmental conditions.

## THEORY OF RANDOM PROCESSES AND SPC

The alternative to classical SPC methods is the method based on the *theory of random processes*. In Barnard's paper[2] the stochastic process of the changes of normally distributed mean $\mu(t)$ is described. In the present article attribute data is considered. The method is to observe and analyse the *dynamics* of non-conforming units appearance, but not the monitoring of their fraction in a sample.

The base integer variable is the number of conforming units $G$† between two consecutive appearances of non-conforming ones. The base variable $G$ is the analogue of the time interval between system transitions into another state (times between events) in the theory of random processes.

Let us describe the process of the appearance of non-conforming units as a Poisson one. Suppose that it is:

(a) ordinary
(b) memoryless
(c) stationary.

In this case variables $G$ are geometrically distributed:

$$p(G) = \bar{p}(1-\bar{p})^G \tag{2}$$

where $p(G)$ is the probability that the first non-conforming unit's appearance will be after exactly $G$ trials according to a Bernoulli sequence.

For $\bar{p} \ll 1$ (<100 ppm) the geometric distribution may be approximated by the exponential one:

$$p(G) = (1/\bar{\bar{G}}) \exp(-G/\bar{\bar{G}}) \tag{3}$$

where $\bar{\bar{G}}$ is the average number of conforming units between two consecutive appearances of non-conforming ones.

There is dependence between statistics of the $G$-chart and the $p$-chart:

$$1/\bar{p} = \bar{\bar{G}} + 1 \tag{4}$$

The result of the Chi-square or Kolmogorov–Smirnov tests for goodness-of-fit to the geometric distribution can be a criterion for the existence of *assignable causes*.

† Here (and further on) the variable $G$ can also be the number of units or the time interval up to the system transition into another state for 'stepped' processes: $G$ = Var = $\{W, T\}$.

## CONTROL LIMITS FOR AN INDIVIDUAL $G$-CHART

Conditions for the definition of control limits according to Shewhart are

$$\alpha_L = \text{Prob}[G < \text{LCL}_G] \tag{5}$$

$$\alpha_U = \text{Prob}[G > \text{UCL}_G] \tag{6}$$

Therefore we have control limits for an *individual* $G$-chart:

$$\text{LCL}_G = -\bar{\bar{G}} \ln(1-\alpha) \tag{7}$$

$$\text{UCL}_G = -\bar{\bar{G}} \ln(\alpha) \tag{8}$$

where the process is defined as a Poisson process.

If the process is not the Poisson, the construction of control limits should be computed for the assumed distribution function instead of the geometric (exponential) distribution.

An example of a process simulated data sheet with $\bar{p}$ = 50 ppm is given in Table I, and an appropriate individual $G$-chart is shown in Figure 1. It can be noted that the individual $G$-chart has low resolution to process changes in the area close to $\text{LCL}_G$.

## $G$-BAR CHART

To increase the sensitivity of the method we should use averages from several $G$ observations, as is done in the classical $X$-bar chart for variables.

Let $k$ be the subgroup size. The averages $\bar{G}$ ($G$-bar) will have a negative binomial distribution with parameter $k$ and for $\bar{p} \ll 1$ may be approximated by the gamma distribution.

The smallest possible value for a lower control limit is $\text{LCL}_G = 1$, therefore

$$p(0) \leq \alpha_L = 0{\cdot}00135 \tag{9}$$

For the geometric ($k = 1$) and negative binomial ($k > 1$) distributions we have

$$\bar{p}^k \leq \alpha_L \quad \text{or} \quad k \geq \log(0{\cdot}00135)/\log(\bar{p}) \tag{10}$$

If $k = 1$, then $\bar{p} \leq 0{\cdot}00135$ (1350 ppm). Since we consider the case $\bar{p} \ll 1$ (< 100 ppm), condition (10) is not critical.

In Table II, factors for control limit determination are given depending on a subgroup size $k$ according to conditions (5), (6) for $\pm$ $3\sigma$.

An example of the $G$-bar chart for $k = 10$ is shown in Figure 2 for data from Table I. The *stabilized* $G/\bar{\bar{G}}$-*chart* is introduced in Appendix I.

## SENSITIVITY OF THE $G$-CHART

Studies of the sensitivity of $G$-charts for the detection of process changes have been implemented by the construction of operating characteristic curves

Table I. Example of a data sheet for a monitored process

| $j$ | $G(j)$ |
|---|---|
| 1 | 9957 |
| 2 | 62,839 |
| 3 | 15,648 |
| 4 | 4399 |
| 5 | 21,512 |
| 6 | 6685 |
| 7 | 14,533 |
| 8 | 18,688 |
| 9 | 30,590 |
| 10 | 15,404 |
| 11 | 30,137 |
| 12 | 13,295 |
| 13 | 9745 |
| 14 | 29,646 |
| 15 | 16,737 |
| 16 | 10,479 |
| 17 | 7709 |
| 18 | 56,046 |
| 19 | 4014 |
| 20 | 3813 |
| 21 | 17,535 |
| 22 | 7943 |
| 23 | 68,234 |
| 24 | 184 |
| 25 | 35,663 |
| 26 | 6784 |
| 27 | 45,497 |
| 28 | 22,063 |
| 29 | 32,513 |
| 30 | 5366 |
| 31 | 22,412 |
| 32 | 1667 |
| 33 | 29,123 |
| 34 | 10,951 |
| 35 | 30,355 |
| 36 | 11,991 |
| 37 | 398 |
| 38 | 25,044 |
| 39 | 13,958 |
| 40 | 10,516 |
| 41 | 6836 |
| 42 | 16,766 |
| 43 | 39,784 |
| 44 | 5555 |
| 45 | 29,082 |
| 46 | 41,777 |
| 47 | 5734 |
| 48 | 34,621 |
| 49 | 30,055 |
| 50 | 9719 |

in Figure 3. Operating characteristic curves for a single-limit $p$-chart have also been plotted in Figure 4 for the same changes of process conditions. As can be noticed from Figures 3 and 4 for the $G$-chart and the $p$-chart with the same sensitivity there is a conformity between the subgroup size $k$ and the parameter $\lambda = n\bar{p}$. This dependence,

$$n\bar{p} = f(k) \tag{11}$$

is shown in Figure 5. For example, the $p$-chart with $\lambda = 3{\cdot}3$ and the $G$-bar chart with subgroup size $k = 10$ have approximately the same sensitivity for detecting process deterioration.

If the individual subgroups are assumed to be independent of each other, then there is a simple equation for average run length (ARL) determination:[3]

$$\text{ARL} = 1/(1-P_a) \tag{12}$$

where $P_a$ is the probability of a subgroup result falling above $\text{LCL}_G$ for the $G$-chart, or the probability of a sample result falling below $\text{UCL}_p$ for the single-limit $p$-chart.

$\text{ARL}_G$ curves for $G$-charts are plotted in Figure 6.

In addition to ARL, two criteria describing *economical* and *dynamic* properties of control charts for the detection of process changes have been implemented. The first criterion is an average number of non-conforming units (ANNU) which appear between the process change and this change detection. The second criterion is an average number of units (ANOU) to be observed between the process change and this change detection. Calculation and comparison of these criteria for the $G$-chart and the single-limit $p$-chart of the same sensitivity are given in Appendix II. Thus, on the average fewer non-conforming units appear, and on the average, fewer units are to be observed for detection of process changes when the $G$-chart is used.

For example, when the process change is from $\bar{p} = 50$ ppm to $p' = 250$ ppm these differences are

$$\text{ANNU}_p - \text{ANNU}_G = 7 \text{ non-conforming units;}$$

$$\text{ANOU}_p - \text{ANOU}_G = 27{,}645 \text{ observed units,}$$

for $k = 10$ and $n\bar{p} = f(10) = 3{\cdot}3$, $n = 66{,}000$.

## OPTIMAL SIZE OF THE SUBGROUP

The 'family' of $\text{ANNU}_G$ charts is given in Figure 7. The bottom bordering curve drawn to this 'family' of charts makes it possible to determine the optimal size $k^*$ of the subgroup for different degrees of process shifts (Figure 8). In this case the average number of non-conforming units will be minimum between the process change and this change detection on the $G$-chart.

For example, if we are interested in the detection of the shift in the process average say to $r = p'/\bar{p} = 5$, the subgroup size $k^* = 8$ should be chosen. Then $\text{ANNU}_G = 9{\cdot}92$ is minimum: $\text{ANNU}_G = 10{\cdot}19$ for $k = 7$ and $\text{ANNU}_G = 10{\cdot}13$ for $k = 9$.

Analogous curves can be plotted for $\text{ANOU}_G$ (Figure 9). It can be noted that the previously obtained optimal subgroup size $k^*$ also provides minimum $\text{ANOU}_G$. In our example $\text{ANOU}_G =$

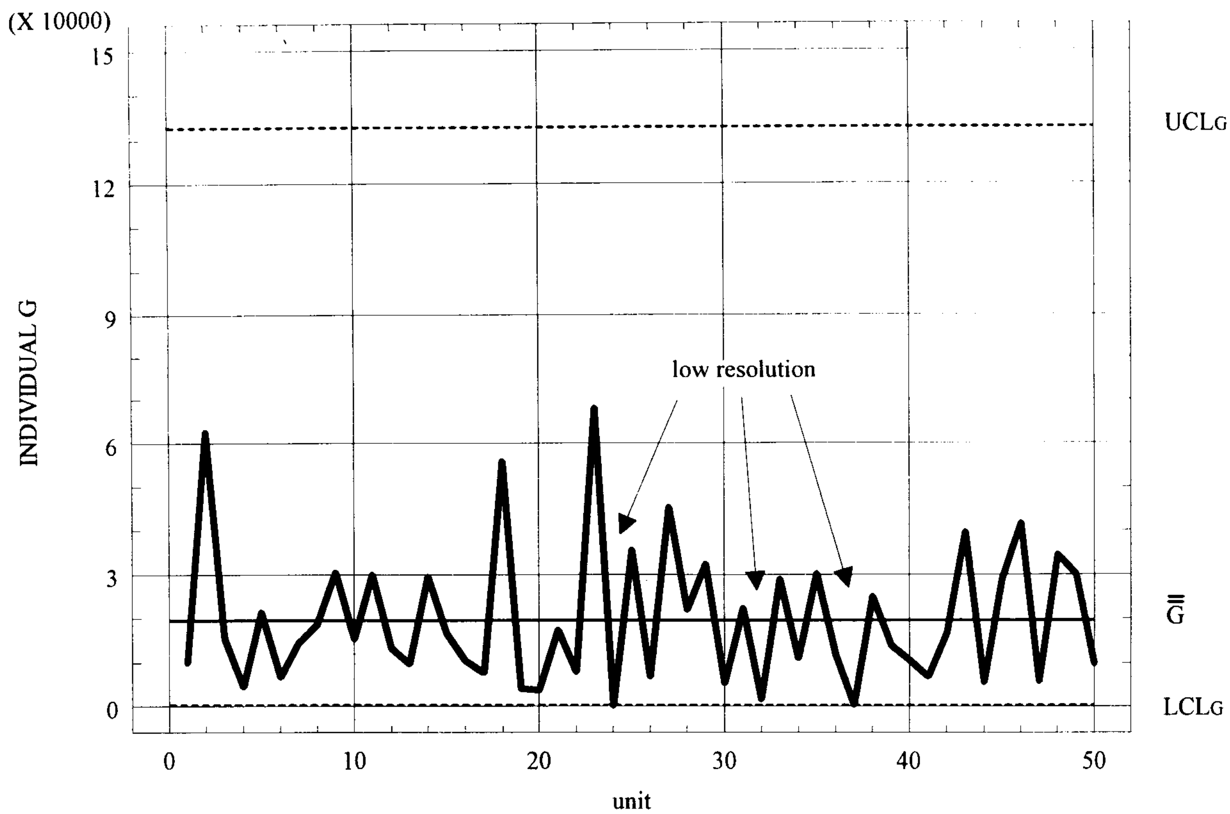


Figure 1. The individual $G$-chart

Table II. Factors for computing control limits for $\pm 3\sigma$

| $k$ | LCL/$\bar{\bar{G}}$ | UCL/$\bar{\bar{G}}$ |
|---|---|---|
| *For individual G-chart* | | |
| 1 | $1{\cdot}35 \times 10^{-3}$ | 6·62 |
| *For G-bar chart* | | |
| 2 | $2{\cdot}64 \times 10^{-3}$ | 4·46 |
| 3 | $7{\cdot}06 \times 10^{-2}$ | 3·63 |
| 4 | 0·116 | 3·18 |
| 5 | 0·158 | 2·88 |
| 6 | 0·196 | 2·68 |
| 7 | 0·229 | 2·51 |
| 8 | 0·258 | 2·41 |
| 9 | 0·285 | 2·29 |
| 10 | 0·308 | 2·24 |
| 11 | 0·331 | 2·17 |
| 12 | 0·349 | 2·11 |

39,700 for $k^* = 8$, whereas $\mathrm{ANOU}_G = 40{,}760$ for $k = 7$ and $\mathrm{ANOU}_G = 40{,}500$ for $k = 9$.

For optimum subgroup size the detection of process changes on the average takes place on the first or second subgroup chosen after the shift has occurred (optimal area in Figure 6). In this case the probability $P_a$ of a subgroup result falling above $\mathrm{LCL}_G$ is about 0·20 (optimal area in Figure 3).

## CONCLUSIONS

1. *On-line control.* Data collection is the record of consecutive appearances of conforming or non-conforming units in the order of production and not their fractions in samples.
2. *Highly informative data.* The data sheet for the classical $p$-chart is a derivative from the $G$-chart data. So based on the $G$-chart data sheet, the $p$-chart can be plotted, and it is impossible to make inverse plotting. In Table III formation of the data sheet for the classical $p$-chart with sample size $n = 66{,}000$ is shown based on the data example of Table I.
3. *Extended application area.* $G$-charts can be employed for those areas where classical SPC for attributes is either problematic or impossible, such as *high quality processes* (with $\bar{p} < 100$ ppm); *low volume manufacturing, short runs* and *'stepped' processes*.
4. *Simple interpretation.* It is possible to carry out usual methods of interpretation on $G$-control charts: *tendency, runs* and *cycling analysis*.
5. *Conformity of parameters.* There is a simple dependence (4) between the statistics of the $G$-chart and the $p$-chart.
6. Compared with the classical $p$-chart of the same sensitivity, the $G$-chart provides *more dynamic, quicker response*, because on the average fewer units are to be observed between the process change and this change detection.

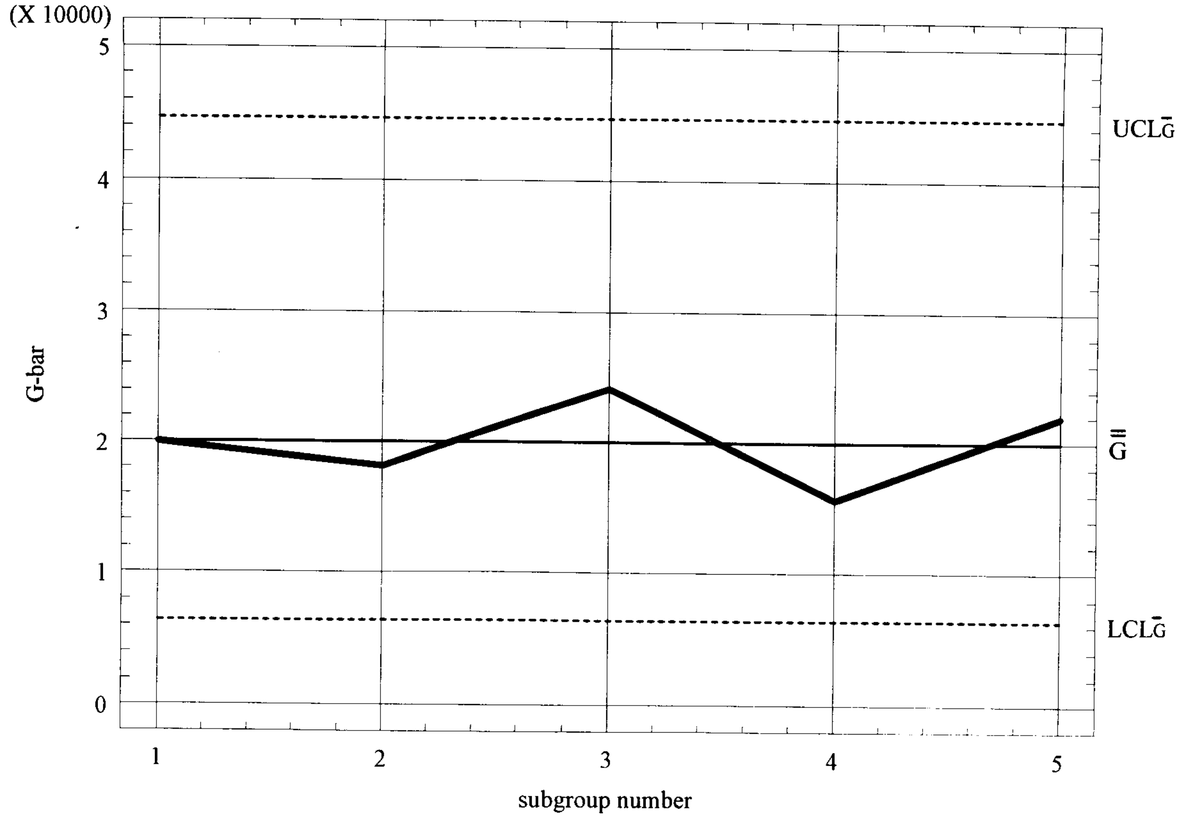


Figure 2. The $G$-bar chart for $k = 10$

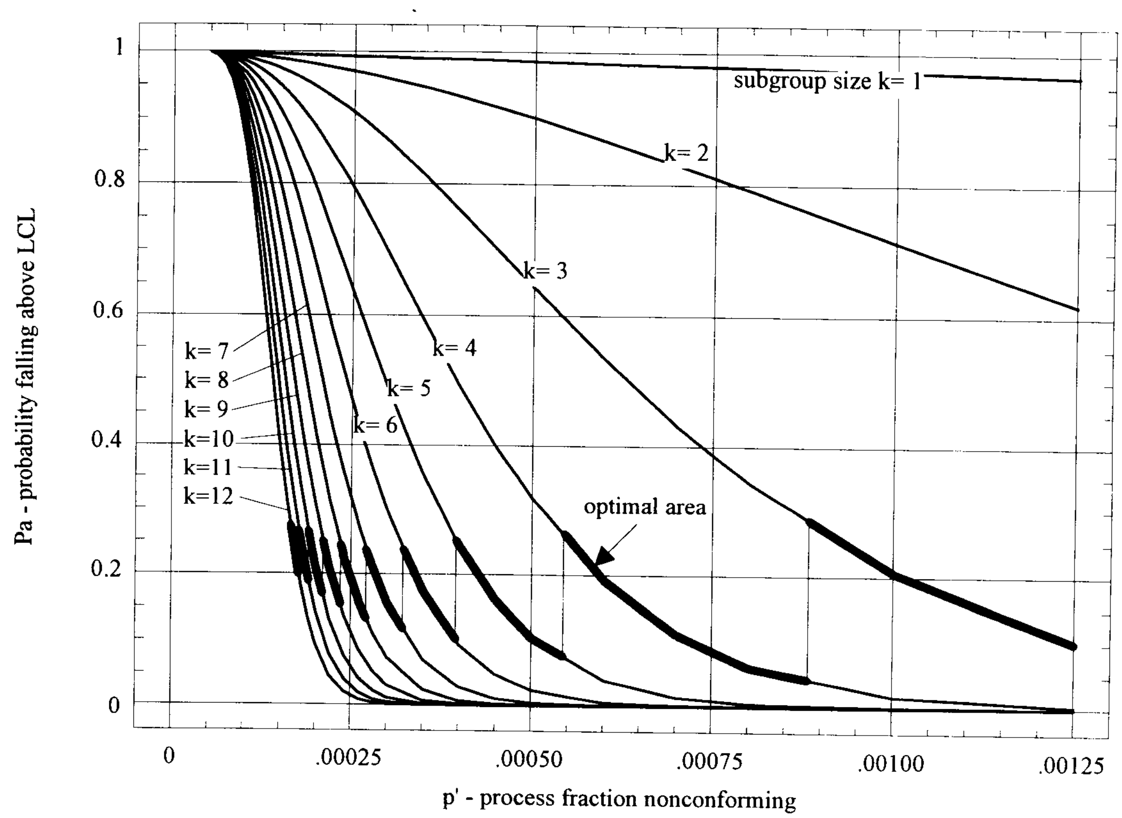


Figure 3. Operating characteristic curves for $G$-charts ($\bar{p}$ = 50 ppm)

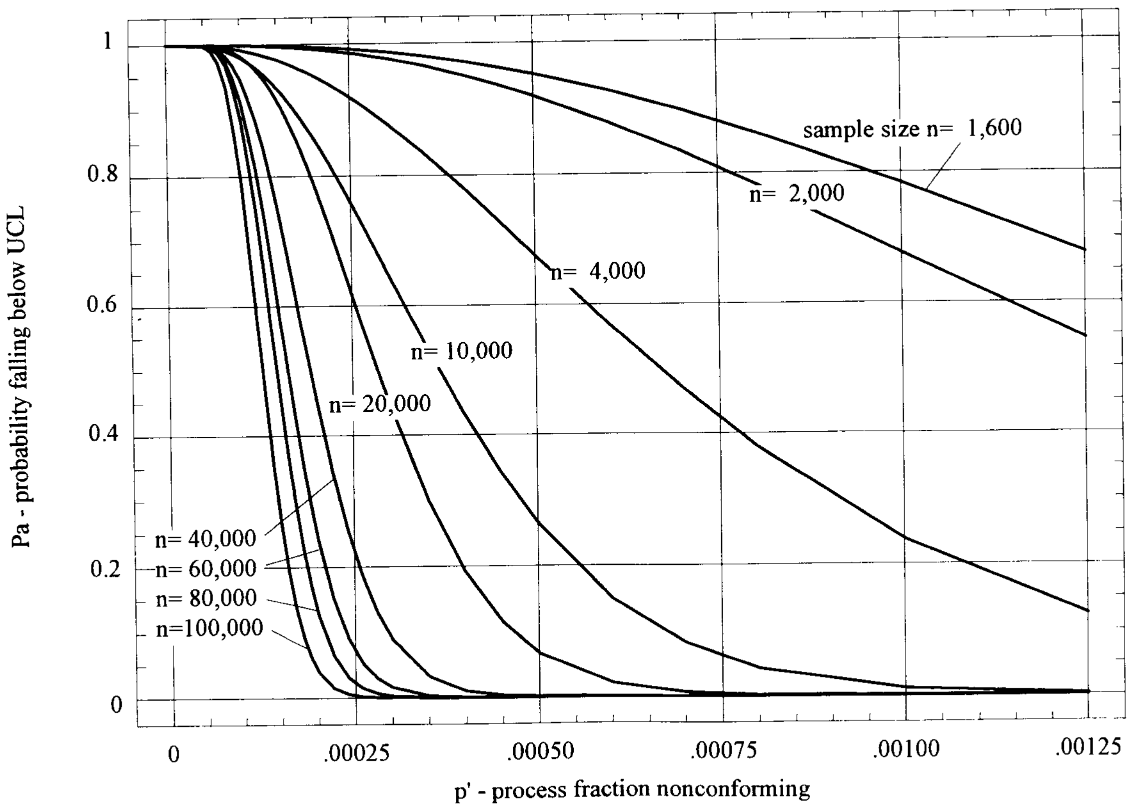


Figure 4. Operating characteristic curves for single-limit $p$-charts ($\bar{p}$ = 50 ppm)

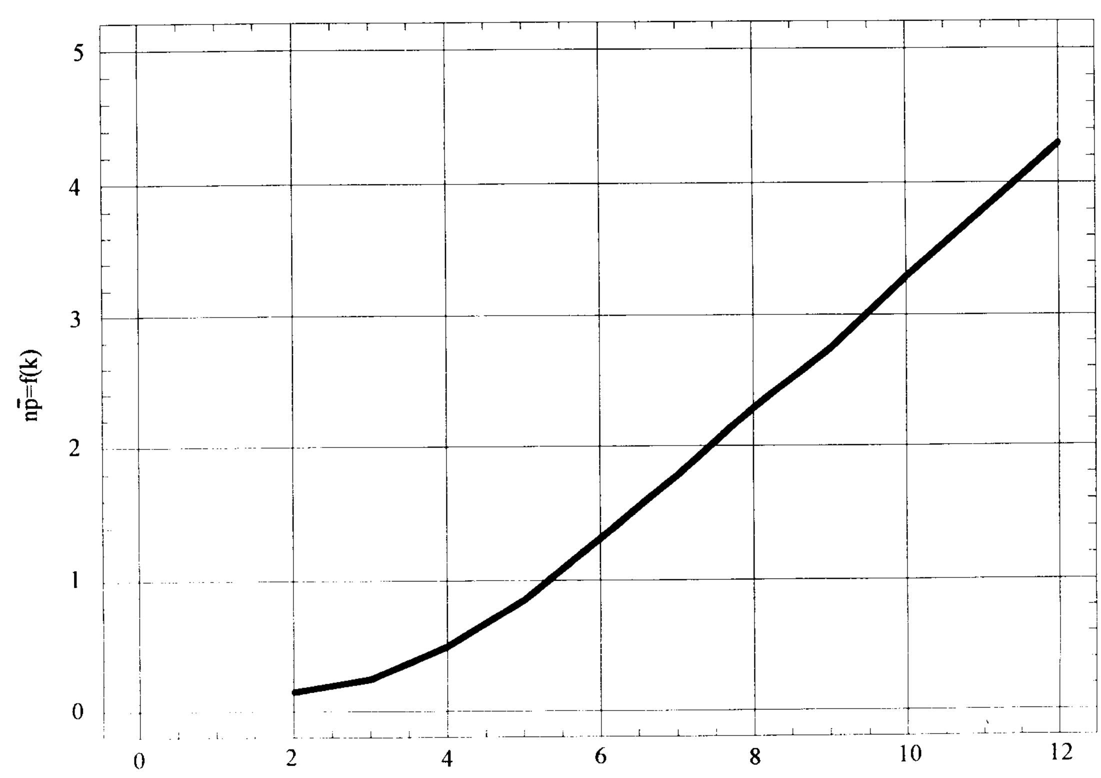


Figure 5. Conformity between subgroup size $k$ for the $G$-chart and the parameter $\lambda = n\bar{p}$ for the $p$-chart with the same sensitivity

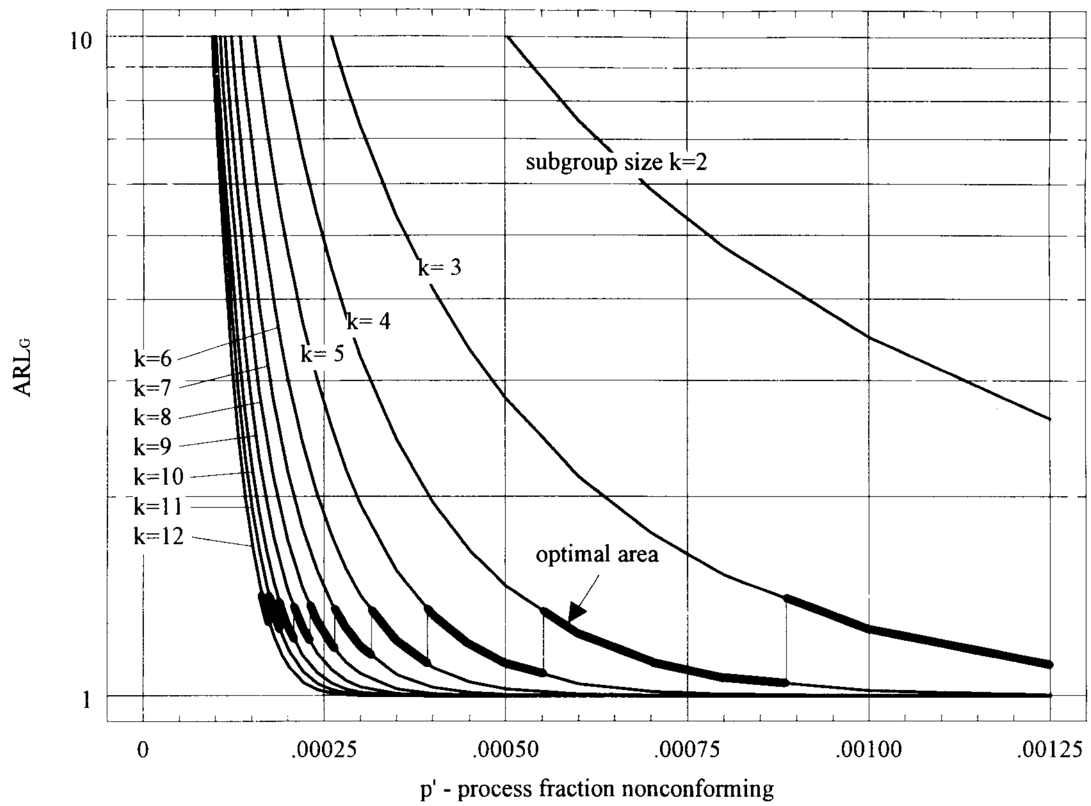


Figure 6. Average run length curves for $G$-charts ($\bar{p}$ = 50 ppm)

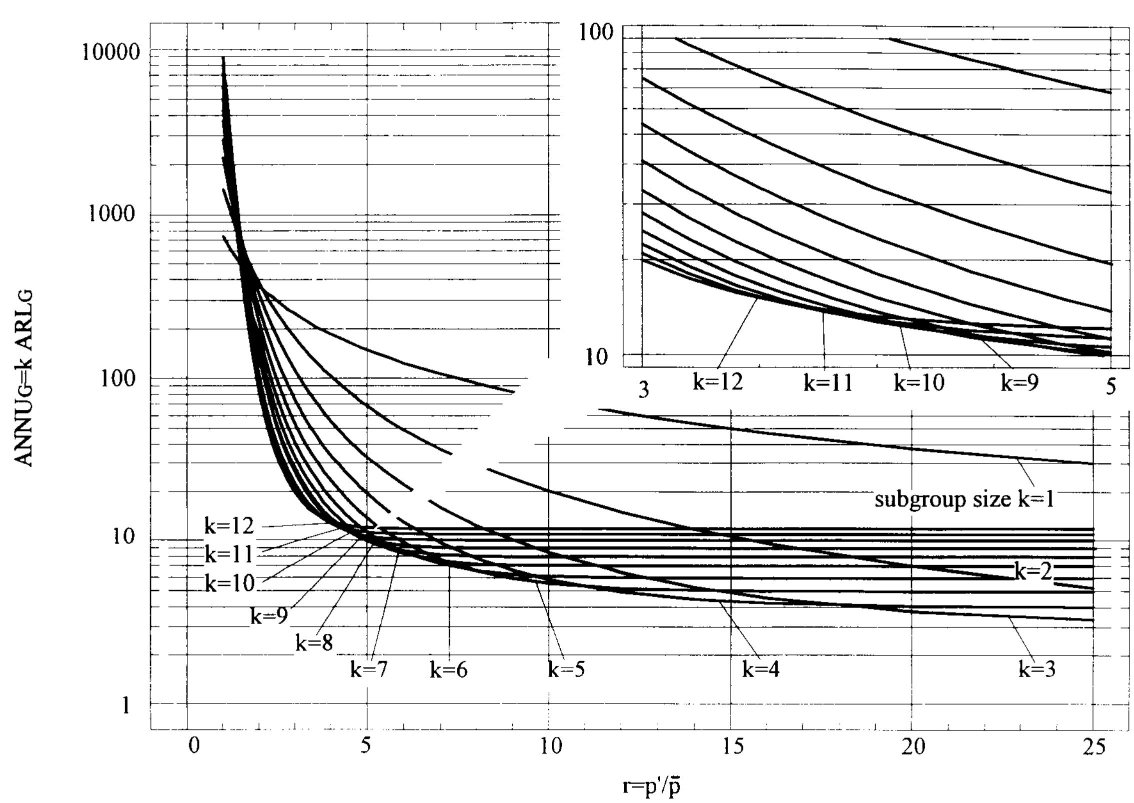


Figure 7. The 'family' of $ANNU_G$ charts

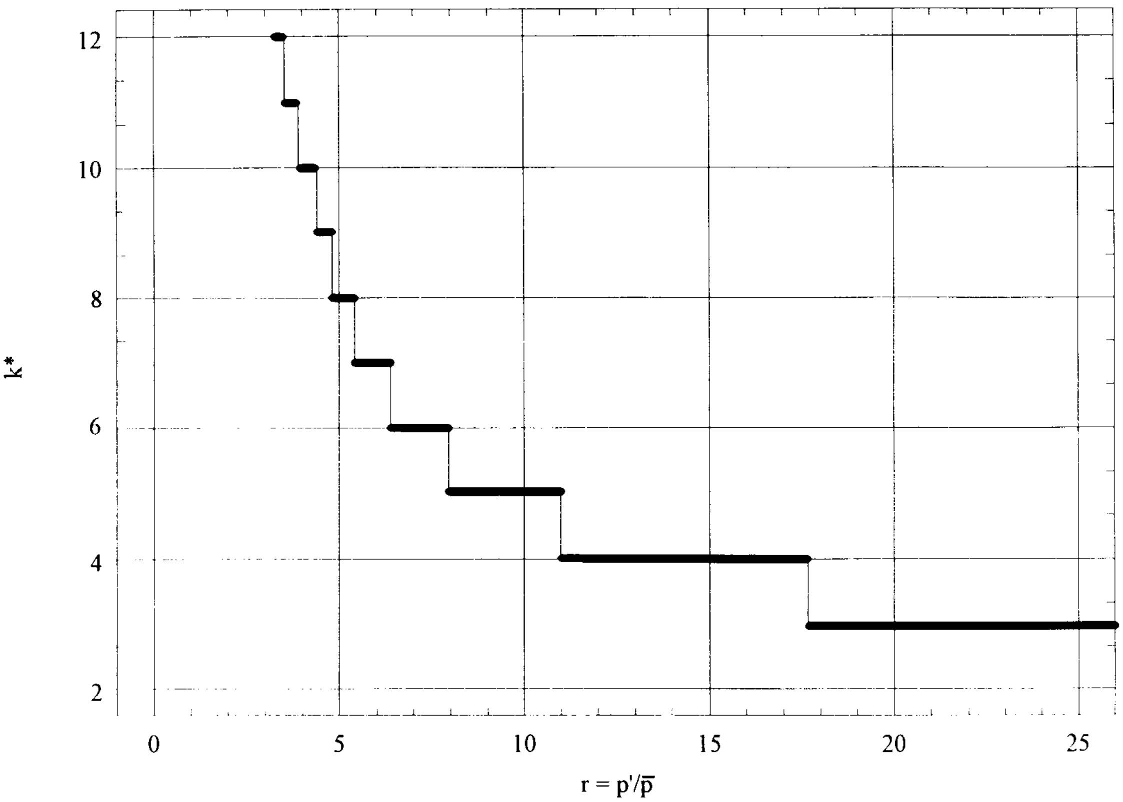


Figure 8. Optimal subgroup sizes $k^*$ for different degress of process shifts $r$

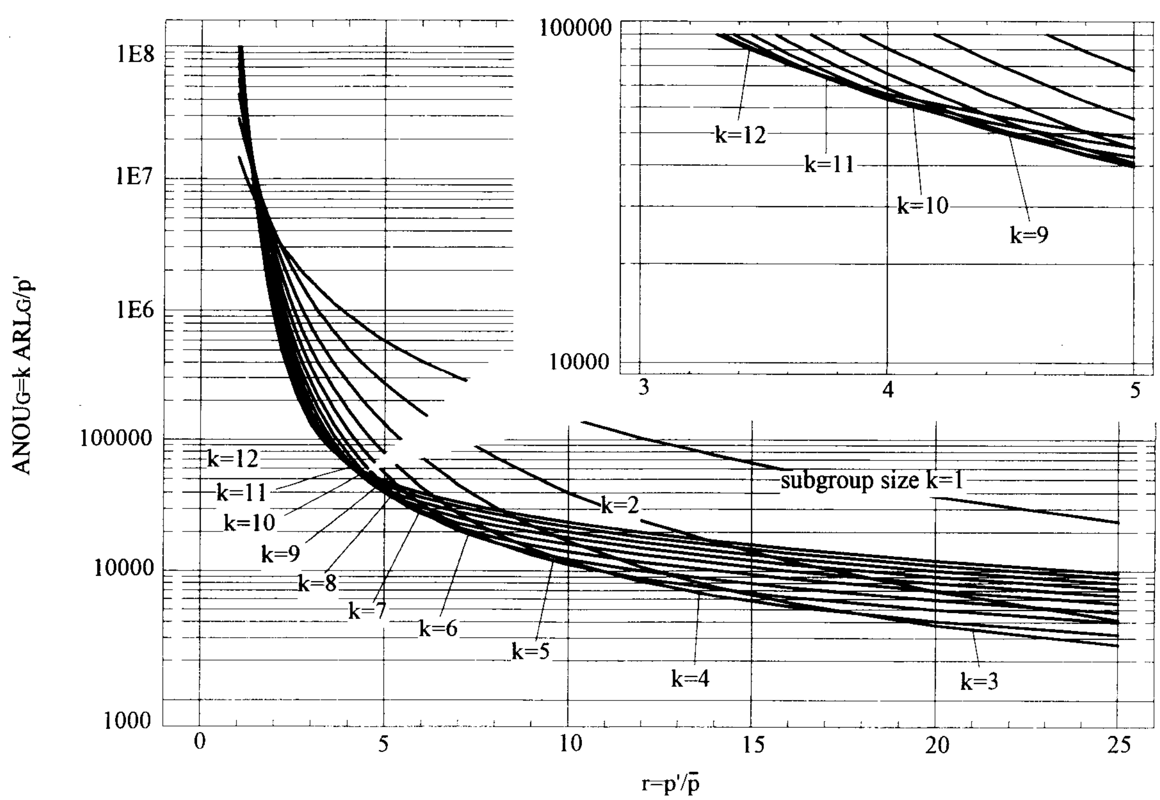


Figure 9. The 'family' of $ANOU_G$ charts

Table III. Construction of a data sheet for the classical $p$-chart based on the data example from Table I

| $j$ | $G(j)$ | CuSum $[G(j)]$ | CuSum $[G(j)+1]$ | $i$ | $np(i)$ |
|---|---|---|---|---|---|
| 1 | 9957 | 9957 | 9958 | 1 | 1 |
| 2 | 62,839 | 72,796 | 72,798 | 2 | 5 |
| 3 | 15,648 | 88,444 | 88,447 | | |
| 4 | 4399 | 92,843 | 92,847 | | |
| 5 | 21,512 | 114,355 | 114,360 | | |
| 6 | 6685 | 121,040 | 121,046 | | |
| 7 | 14,533 | 135,573 | 135,580 | 3 | 3 |
| 8 | 18,688 | 154,261 | 154,269 | | |
| 9 | 30,590 | 184,851 | 184,860 | | |
| 10 | 15,404 | 200,255 | 200,265 | 4 | 4 |
| 11 | 30,137 | 230,392 | 230,403 | | |
| 12 | 13,295 | 243,687 | 243,699 | | |
| 13 | 9745 | 253,432 | 253,445 | | |
| 14 | 29,646 | 283,078 | 283,092 | 5 | 4 |
| 15 | 16,737 | 299,815 | 299,830 | | |
| 16 | 10,479 | 310,294 | 310,310 | | |
| 17 | 7709 | 318,003 | 318,020 | | |
| 18 | 56,046 | 374,049 | 374,067 | 6 | 3 |
| 19 | 4014 | 378,063 | 378,082 | | |
| 20 | 3813 | 381,876 | 381,896 | | |
| 21 | 17,535 | 399,411 | 399,432 | 7 | 2 |
| 22 | 7943 | 407,354 | 407,376 | | |
| 23 | 68,234 | 475,588 | 475,611 | 8 | – |
| 24 | 184 | 475,772 | 475,796 | | |
| 25 | 35,663 | 511,435 | 511,460 | | |

In this case there is also *economic control* since on the average fewer non-conforming units appear.

## APPENDIX I. STABILIZED $G/\bar{\bar{G}}$-CHART

The variable coding

$$\tilde{G} = G/\bar{\bar{G}} \tag{13}$$

makes it possible to plot a *stabilized* $G/\bar{\bar{G}}$ control chart[3] both for individual $G$-charts and for $G$-bar charts. In this case control limits do not depend upon $\bar{\bar{G}}$ and are determined directly from Table II by the value $k$ for $\bar{\bar{G}} = 1$. So for $k = 10$, $\mathrm{LCL}_{\bar{G}} = 0{\cdot}308$, $\mathrm{UCL}_{\bar{G}} = 2{\cdot}24$, central line $= 1$.

An example of the stabilized $G/\bar{\bar{G}}$-bar chart is depicted in Figure 10 for data from Table I (compare with the $G$-bar chart in Figure 2).

## APPENDIX II. CALCULATION AND COMPARISON OF ANNU AND ANOU FOR A $G$-CHART AND A SINGLE-LIMIT $p$-CHART OF THE SAME SENSITIVITY

For the $G$-chart and the single-limit $p$-chart with the same sensitivity we have:

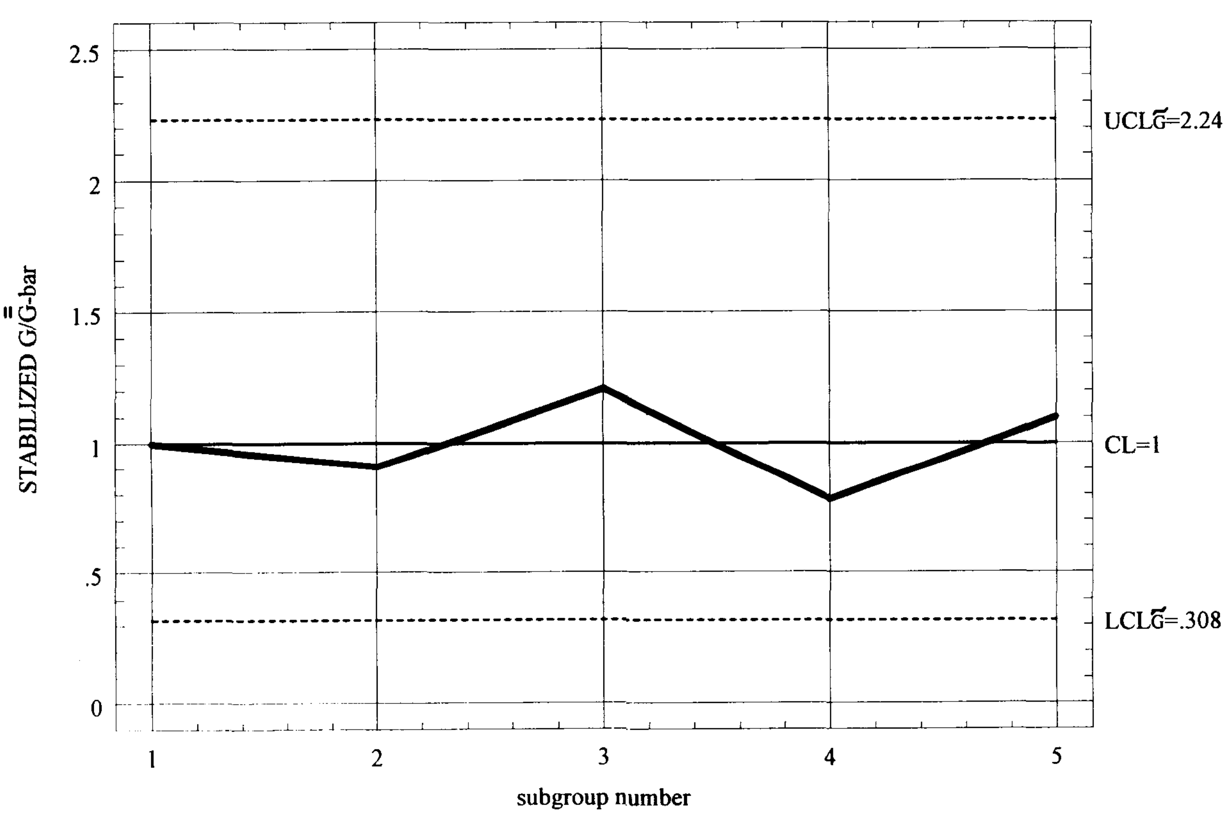


Figure 10. The stabilized $G/\bar{\bar{G}}$-bar chart for $k = 10$

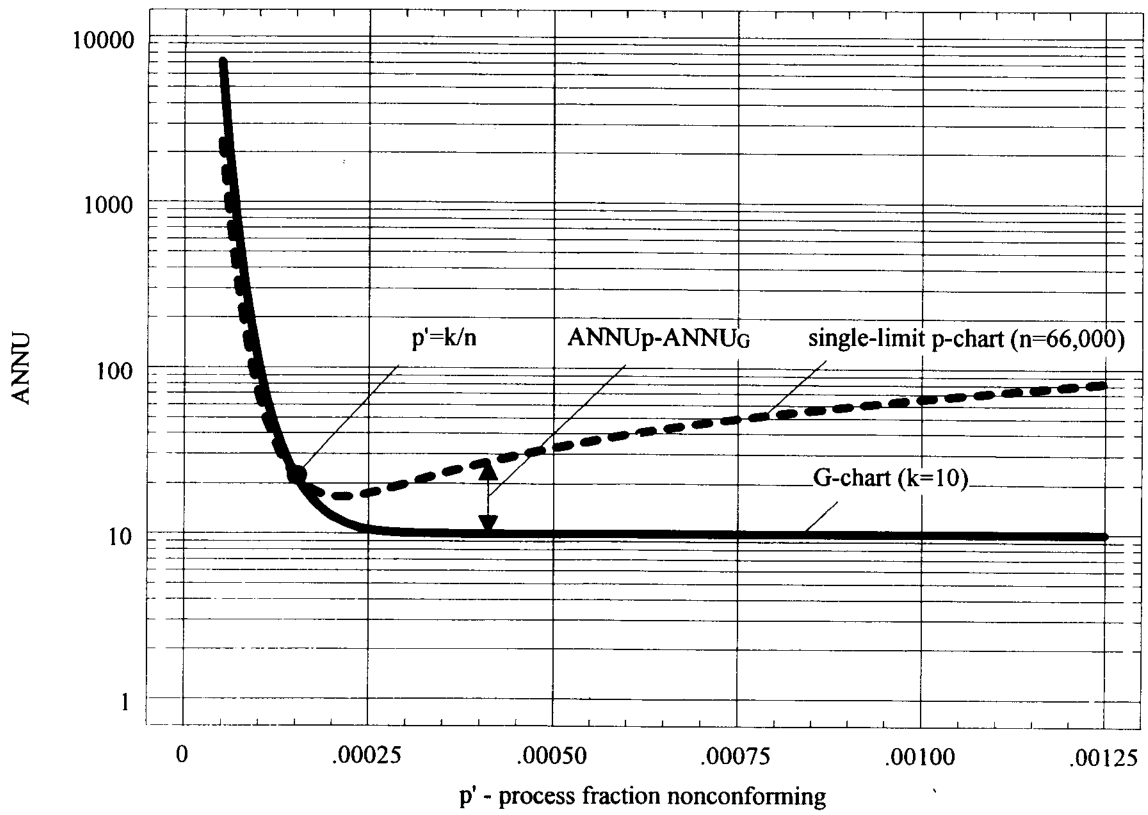


Figure 11. Comparison of the values of $ANNU_G$ for $k = 10$ and $ANNU_p$ for $n\bar{p} = 3{\cdot}3$ ($\bar{p} = 50$ ppm)

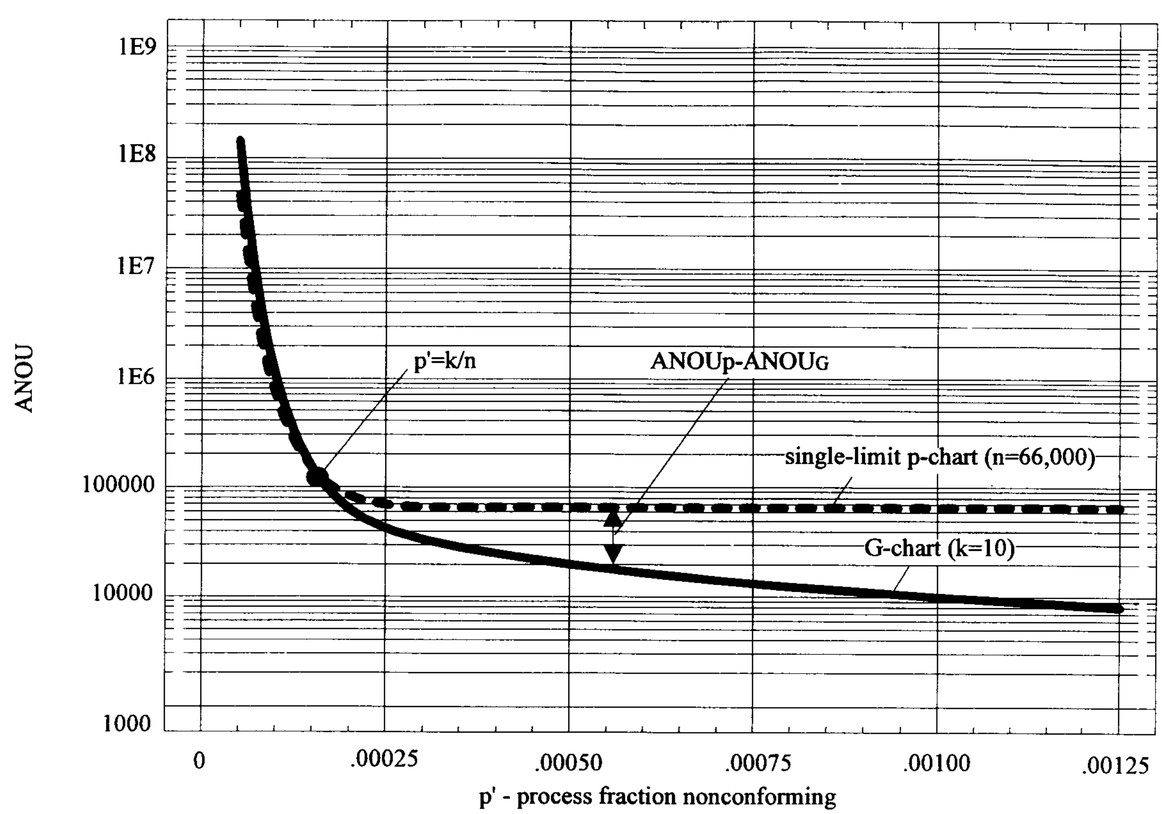


Figure 12. Comparison of the values of $ANOU_G$ for $k = 10$ and $ANOU_p$ for $n\bar{p} = 3{\cdot}3$ ($\bar{p} = 50$ ppm)

$$\mathrm{ANNU}_G = k\,\mathrm{ARL}_G\,(r; k),\ r = p'/\bar{p} \qquad (14)$$

$$\begin{aligned}\mathrm{ANNU}_p &= np'\,\mathrm{ARL}_p\,(r; n\bar{p})\\ &= rf(k)\,\mathrm{ARL}_G\,(r; k) \qquad (15)\end{aligned}$$

A comparison of the values of $\mathrm{ANNU}_G$ for $k$ = 10 and $\mathrm{ANNU}_p$ for $n\bar{p} = f(10) = 3{\cdot}3$ is given in Figure 11.

The average number of observed units between the process change and this change detection on the $G$-chart is

$$\begin{aligned}\mathrm{ANOU}_G &= k\,\mathrm{ARL}_G\,(r; k)/p'\\ &= k\,\mathrm{ARL}_G\,(r; k)/(r\bar{p}) \qquad (16)\end{aligned}$$

and on the single-limit $p$-chart with the same sensitivity it is consequently

$$\begin{aligned}\mathrm{ANOU}_p &= n\,\mathrm{ARL}_p\,(r; n\bar{p})\\ &= f(k)\,\mathrm{ARL}_G\,(r; k)/\bar{p} \qquad (17)\end{aligned}$$

A comparison of the values of $\mathrm{ANOU}_G$ for $k$ = 10 and $\mathrm{ANOU}_p$ for $n\bar{p} = f(10) = 3{\cdot}3$ is given in Figure 12.

The difference $\mathrm{ANNU}_p - \mathrm{ANNU}_G$ between the ordinates in Figure 11 and the difference $\mathrm{ANOU}_p - \mathrm{ANOU}_G$ between the ordinates in Figure 12 illustrate the priority of the $G$-chart compared with the single-limit $p$-chart with the same sensitivity for detection of process changes to $p' > k/n = \bar{p}k/f(k)$. To detect slight changes of the process to $p' \leq k/n$ the adjustment of subgroup size $k$ in conformity with the 'Optimal size of the subgroup' section should be made.

## REFERENCES


1. C. P. Quesenberry, 'SPC $Q$-charts for a binomial Parameter $\bar{p}$: short or long runs', *Journal of Quality Technology*, **23**, 239–246 (1991).
2. G. A. Barnard, 'Control charts and stochastic processes', *Journal of the Royal Statistical Society, Series B*, **XXI**, (2), 239–257 (1959).
3. A. J. Duncan, *Quality Control and Industrial Statistics*, 5th edn, Richard D. Irwin, Homewood, IL, 1986.


*Author's biography:*

**Eli A. Glushkovsky** is a Statistical Quality Control Manager at Telrad Telecommunication and Electronic Industries Ltd., Israel. He received his M.S. in electrical engineering and his doctorate in mathematical simulation of technological processes, both of them from the St Petersburg Institute of Technology, Russia. His areas of research include mathematical simulation and optimization of technological processes, design of experiments and process control. He is a member of ASQC and ISQ, CQE and CRE.